Ovarian Expression of Insulin-Like Peptide 3 (INSL3) and Its Receptor (RXFP2) During Development of Bovine Antral Follicles and Corpora Lutea and Measurement of Circulating INSL3 Levels During Synchronized Estrous Cycles

Leanne Satchell, Claire Glister, Emma C. Bleach, Richard G. Glencross, Andrew B. Bicknell, Yanzhenzi Dai, Ravinder Anand-Ivell, Richard Ivell, and Philip G. Knight

School of Biological Sciences (L.S., C.G., R.G.G., A.B.B., P.G.K.), University of Reading, Whiteknights, Reading RG6 6UB, United Kingdom; Animal Production (E.C.B.), Welfare and Veterinary Sciences Department, Harper Adams University College, Newport TF10 8NB, Shropshire, United Kingdom; and Leibniz Institute for Farm Animal Biology (Y.D., R.A.-I., R.I.), 18196 Dummerstorf, Germany

Insulin-like peptide 3 (INSL3), a major product of testicular Leydig cells, is also expressed by the ovary, but its functional role remains poorly understood. Here, we quantified expression of *INSL3* and its receptor *RXFP2* in theca interna cell (TIC) and granulosa cell compartments of developing bovine antral follicles and in corpora lutea (CL). *INSL3* and *RXFP2* mRNA levels were much higher in TIC than granulosa cell and increased progressively during follicle maturation with *INSL3* peaking in large (11-18 mm) estrogen-active follicles and *RXFP2* peaking in 9- to 10-mm follicles before declining in larger (11-18 mm) follicles. Expression of both *INSL3* and *RXFP2* in CL was much lower than in TIC. In situ hybridization and immunohistochemistry confirmed abundant expression of *INSL3* mRNA and protein in TIC. These observations indicate follicular TIC rather than CL as the primary site of both INSL3 production and action, implying a predominantly autocrine/paracrine role in TIC. To corroborate the above findings, we showed that in vitro exposure of TIC to a luteinizing concentration of LH greatly attenuated expression of both INSL3 and its receptor while increasing progesterone secretion and expression of *STAR* and *CYP11A1*. Moreover, in vivo, a significant cyclic variation in plasma INSL3 was observed during synchronized estrous cycles. INSL3 and estradiol-17β followed a similar pattern, both increasing after luteolysis, before falling sharply after the LH surge. Thus, theca-derived INSL3, likely from the dominant preovulatory follicle, is detectable in peripheral blood of cattle, and expression is down-regulated during luteinization induced by the preovulatory LH surge. Collectively, these findings underscore the likely role of INSL3 as an important intrafollicular modulator of TIC function/steroidogenesis, while raising doubts about its potential contribution to CL function. (*Endocrinology* 154: 1897–1906, 2013)

Insulin-like peptide 3 (INSL3) is a member of the relaxin-insulin family of peptide hormones and is a major secretory product of the testicular Leydig cells of male mammals (1–3). In the adult male, it is produced in large quantities, in a constitutive manner, and gives rise to substantial concentrations in the peripheral circulation. It is a good marker for fully differentiated Leydig cells and is likely to play a role in maintaining spermatogenesis (2). In the male fetus, INSL3 is an important product of the fetal Leydig cells and is instrumental in the transabdominal phase of testicular descent (4). Hence, the principal phenotype of male *Insl3* knockout mice is primary cryp-

torchidism (5, 6). INSL3 signals through a G protein-coupled receptor known as relaxin family peptide receptor (RXFP)2 (7), which is closely related to the relaxin receptor RXFP1. Mice lacking RXFP2 exhibit the same cryptorchid phenotype as that of *Insl3* knockout mice (8, 9).

Although INSL3 has principally been described as a male hormone, it is also expressed in the adult female, by follicular theca cells and corpus luteum (CL) of the ovary (10–16). The role of INSL3 in the female is not well defined. However, there is evidence to suggest that it is involved in postpubertal follicular selection and maturation. INSL3 knockout mice have been found to display impaired fertility and have higher rates of follicular atresia and fewer ovulations than their wild-type littermates (5, 17). It has been suggested that INSL3 is a marker of differentiated theca cells and can be modulated by factors that influence follicle differentiation, such as IGF, insulin, and LH (14, 18). Levels have also been shown to decline in atretic follicles (14).

INSL3 has been detected in the peripheral blood of adult women but at much lower levels than in men (19, 20), perhaps indicating that it plays a local intraovarian role rather than a systemic endocrine role in the female (2). However, in ruminants, ovarian expression levels are considerably higher than in other mammals, and this may indicate that it also plays a systemic role in these species (11, 18).

The aims of the present study were, firstly, to perform a detailed analysis of the expression of INSL3 and its receptor RXFP2 in bovine ovarian follicles, spanning key stages of antral follicle development, including cyclic recruitment, selection/deviation, luteinizing hormone/choriogonadotropin receptor (LHCGR) acquisition, and dominance, in order to further define the role of INSL3 during follicle development and to identify the target of its action. Secondly, we examined expression of INSL3 and RXFP2 in luteal tissue. Thirdly, bovine theca interna cells (TICs) in primary culture were used to determine the effect of LH-induced luteinization on expression of INSL3 and RXFP2. Finally, circulating plasma levels of INSL3 throughout the bovine oestrus cycle were measured for the first time using a recently developed time-resolved fluorescence immunoassay (21) in order to examine whether there is cyclic variation in INSL3 and to correlate this information with the results from the above-mentioned follicular expression profiling and in vitro experimentation.

Materials and Methods

Bovine ovaries

Ovaries from nonpregnant adult cattle slaughtered at random stages of the estrous cycle were collected from a local abattoir.

They were transported to the laboratory in medium-199 supplemented with 1% (vol/vol) antibiotic antimycotic solution. For in situ hybridization, ovaries were snap frozen in isopentane on dry ice immediately after collection. For immunohistochemistry, fresh follicular tissues were immersion fixed in Bouin's fixative for 6 hours, followed by graded ethanols and embedding in paraffin wax. As control tissues, testis fragments from sexually mature animals were similarly processed.

Preparation of granulosa cell (GC) and TIC extracts for gene expression analysis

Follicles ranging in diameter from 1 to 18 mm were dissected from ovaries that were judged to be from cattle in the mid to late-luteal phase, as described in detail elsewhere (22). Estimation of cycle stage was based on the morphological appearance of the CL (23). Follicles were sorted by size, and their GC, TIC layers, and follicular fluid were recovered. Isolated GCs and TICs were homogenized in 0.5 mL of Trireagent (Sigma UK Ltd, Poole, United Kingdom) and stored at −80°C before RNA extraction. Concentrations of estradiol-17β (E2) and progesterone in follicular fluid were determined by immunoassay. Follicles in the largest size category (11–18 mm) were subdivided according to their follicular fluid E2 to progesterone (P4) ratio, with those with E2 to P4 ratio more than 1 being presumed healthy, "estrogen-active" dominant follicles, and those with E2 to P4 ratio less than 1 being presumed to be "estrogen inactive" and regressing (22).

Isolation of CL samples for gene expression analysis

Samples of CL tissue were isolated from the ovaries and were categorized as being "early-luteal," "midluteal," and "late-luteal" phase, according to the criteria described by Ireland et al (23). CL samples were snap frozen on dry ice and stored at −80°C before subsequent RNA extraction using Trireagent.

In vitro TIC luteinization model

TICs were isolated from the ovaries as described previously (24). For each experiment, TICs were pooled from around 50 follicles of 4–6 mm in diameter and were plated at a density of 500 000 viable cells/well in 24-well plates (Nunclon, Life Technologies Ltd, Carlsbad, California). Serum-free culture medium was used throughout: McCoy's 5A with 1% (vol/vol) antibiotic-antimycotic solution, 10-ng/mL bovine insulin, 2mM L-glutamine, 10mM HEPES, 5-mg/mL apotransferrin, 5-ng/mL sodium selenite, and 0.1% (wt/vol) BSA. Cells were cultured for 6 days (removing and replacing with fresh media every 48 h) at 38.5°C in the presence or absence of a luteinizing dose level (1.5 ng/mL) of ovine LH (NIADDK oLH-S16; obtained from NHPP, Torrance, California). At the end of the culture, conditioned media were retained for P4 and INSL3 immunoassays, and cell lysates were prepared using the lysis buffer supplied with the RNeasy extraction kit (Buffer RLT; QIAGEN Ltd, Manchester, United Kingdom), according to the manufacturer's instructions. Lysates from replicate wells were pooled and stored at −80°C before RNA extraction. The experiment was repeated 4 times with independent batches of ovaries.

In vivo studies in prostaglandin (PG)-synchronized heifers

The 5 British Friesian heifers (~2 y old; ~400-kg body weight) used in this study were housed indoors, loosely tethered in individual stands. They were fed a maintenance ration of concentrates and straw and had continual access to water. Estrous cycles were synchronized by giving 3 injections (im) of the PG $F_{2\alpha}$ analog cloprostenol (0.5 mg), 14 days apart. The day of the third PG injection was designated as day 0 of the study. Two further PG injections were given on days 14 and 28 to induce luteolysis, resulting in 3 truncated cycles being studied per cow (n = 15 cycles in total). Blood samples (50 mL) were taken on a daily basis via a jugular vein catheter that was flushed with sterile 0.9% wt/vol saline containing sodium heparin (100 IU/mL) after sample withdrawal. Samples were collected into polypropylene tubes containing 50 μL of sodium heparin (5000 IU/mL). After centrifugation (2000g for 30 min), plasma was decanted and stored at −20°C awaiting hormone analysis. The experiment was carried out in full compliance with United Kingdom Home Office guidelines and the Animals (Scientific Procedures) Act 1986.

Does E2 directly alter expression of INSL3 or RXFP2 expression by nonluteinized TIC?

To test whether direct exposure on nonluteinized TIC to E2 could affect expression of mRNAs for INSL3 or RXFP2, isolated TICs were cultured with a concentration of LH (150 pg/mL) conducive to optimal androstenedione secretion (24) in the presence and absence of E2 at a concentration (500 ng/mL) comparable with that present in follicular fluid from preovulatory bovine follicles. At the end of culture, conditioned media were retained for androstenedione assay and cell lysates prepared for RNA extraction and real-time PCR analysis. The experiment was repeated 4 times with cells from independent batches of ovaries.

E2, P4, and androstenedione immunoassays

Plasma E2 concentrations were determined by RIA as described previously (25, 26), with an assay detection limit of 1.7 pg/mL and intra- and interassay coefficients of variation of 11% and 15%, respectively. Concentrations of P4 in plasma and cell-conditioned culture media were determined by direct ELISA (27–29). Intra- and interassay coefficients of variation were 9% and 13%, respectively, and the detection limit was 20 pg/mL. Plasma androstenedione levels were measures by ELISA as described elsewhere (30). Before analysis, androstenedione was extracted from the plasma using ethyl ether. Briefly, 5 volumes of ethyl ether were added to 500-μL plasma in glass tubes. Tubes were vortexed for 1 minute and left to stand for 10 minutes to allow

the 2 phases to separate. The upper ethyl ether phase was transferred to a clean glass tube and allowed to evaporate to dryness. The extracted steroid was then redissolved in assay diluent (PBS containing 0.1% wt/vol gelatin and 0.05% vol/vol Proclin 300). Androstenedione standards were made up in charcoal-stripped cow plasma and were ether extracted in parallel with experimental plasma samples. Androstenedione levels in the extracted samples were then measured by competitive ELISA (30), using the extracted standards to calibrate the assay, hence avoiding the need to correct for recoveries. The goat antiandrostenedione antibody (IR637) used in the assay was kindly provided by Dr G. S. Pope (Institute for Grassland and Environmental Research, Hurley, United Kingdom), and androstenedione-horseradish peroxidase conjugate was purchased from Cal Bioreagents (Los Angeles, California). Intra- and interassay coefficients of variation were 7% and 12%, respectively.

INSL3 assay

Concentrations of INSL3 in plasma and TIC-conditioned media were determined using a novel time-resolved fluorescence immunoassay, which is highly specific for ruminant INSL3 and is described in detail elsewhere (21). As tracer for the assay, synthetic bovine INSL3 (A-chain/B-chain heterodimer) was labeled with (Eu^{3+}) chelate (see Supplemental Table 1, published on The Endocrine Society's Journals Online web site at http://endo.endojournals.org). The assay detection range was from 0.02 to 20.0 ng/mL of bovine INSL3. Intra- and interassay coefficients of variation were 2% and 10%, respectively.

RNA isolation

Total RNA was isolated from TIC lysates using the RNeasy kit (QIAGEN Ltd), according to the manufacturer's instructions and the RNA eluted in 30 μL of nuclease-free water. On-column deoxyribonuclease (DNase) digestion was performed using ribonuclease-free DNase (QIAGEN Ltd) to remove any potential DNA contamination. Total RNA was isolated from ex vivo GC, TIC, and CL samples, using Trireagent (Sigma UK Ltd), as described previously (22, 31), and potential genomic DNA contamination was removed with an ribonuclease-free DNase kit (RQ1; Promega UK Ltd, Southampton, United Kingdom). RNA quantity and quality were evaluated by spectrophotometry at 260/280 nm.

cDNA synthesis and real-time PCR

cDNA was synthesized from 1 μg of RNA using the Reverse-iT RT kit (Abgene, Epsom, United Kingdom) according to the manufacturer's instructions. Primers (see Table 1) were designed using Primer Express software (version 1.5; PerkinElmer-Applied Biosystems, Warrington, United Kingdom) and primer-

Table 1.   List of Primers Used for Real-Time PCR

Target	Accession number	Forward primer 5′ to 3′	Reverse primer 5′ to 3′	Amplicon size (base pairs)
STAR	NM_174189	TTTTTTCCTGGGTCCTGACAGCGTC	ACAACCTGATCCTTGGGTTCTGCACC	103
CYP11A1	NM_176644	CAGTGTCCCTCTGCTCAACGTCC	TTATTGAAAATTGTGTCCCATGCGG	99
INSL3	NM_174365.2	TCTGTCCCCACTGAATCCTCCTGG	GGGTTTCATGGTGCTGTGTGGC	102
RXFP2	XR_028620.2	CGAGGGCAGTATCAGAAGTACGCGC	AGACCTCAGTGGACAGCATGGCC	91
ACTB	NM_173979.3	ATCACCATCGGCAATGAGCGGTTC	CGGATGTCGACGTCACACTTCATGA	128

BLAST used to check in silico that no known bovine off-target sequences would be amplified. Primer pairs were also validated using agarose gel electrophoresis to demonstrate amplification of a single product of the predicted size. In addition, post-PCR dissociation curve analyses confirmed the amplification of a single product in each sample. PCR amplification efficiencies for *ACTB*, *INSL3*, *RXFP2*, *STAR*, and *CYP11A1* were 97%, 100%, 100%, 92%, and 93%, respectively. PCR assays were carried out in a total reaction volume of 14 μL, comprising 5-μL cDNA template, 1 μL of each forward and reverse primer (final concentration 0.36μM) and 7-μL QuantiTect SYBR Green qPCR 2$\times$ Master Mix (QIAGEN Ltd). Samples were processed on an AB StepOne Plus real-time PCR instrument (Life Technologies, Paisley, United Kingdom) with cycling conditions: 15 minutes at 95°C (1 cycle only) followed by 15 seconds at 95°C and 1 minute at 60°C for 40 cycles. The relative abundance of each mRNA transcript was compared using the $\Delta\Delta$Ct method (32). Threshold cycle (Ct) values for each transcript in a given sample were first normalized to the β-actin Ct value. It was confirmed that β-actin was a suitable reference control gene because Ct values ($\sim$16 cycles) were uniform across follicle size categories and cell types ($P > .1$; data not shown). For GC, TIC, and CL samples, the resultant ΔCt values were then normalized to the mean ΔCt value for the transcript in all the samples (ie, to generate $\Delta\Delta$Ct values). For TIC culture experiments, ΔCt values for the samples treated with LH (1.5 ng/mL) were normalized to the untreated control samples to generate $\Delta\Delta$Ct values. $\Delta\Delta$Ct values were subsequently converted to fold differences, for graphical presentation, using the formula: fold difference = $2^{-\Delta\Delta Ct}$.

In situ hybridization

Frozen sections (25 μm) were cut using a cryostat, thaw mounted, and stored at -80°C until required. For in situ hybridization sense and antisense riboprobes labeled with digoxygenin were synthesized by in vitro transcription with T7 and T3 RNA polymerase (Promega, Madison, Wisconsin) from nucleotides 96-431 of the *INSL3* gene (accession number NM_174365) cloned into pBluescript (Stratagene, La Jolla, California). After synthesis, the probes were checked for integrity by denaturing gel electrophoresis and purified using the RNeasy kit (QIAGEN Ltd). Frozen slides were rapidly thawed and fixed for 20 minutes in 4% (wt/vol) paraformaldehyde in PBS at 4°C. After proteinase K treatment (20 min at 37°C), sections were hybridized overnight at 65°C with either the sense or antisense riboprobe. After washing the sections, hybridized probe was detected using an alkaline phosphatase-conjugated antidigoxygenin antibody and visualized using NBT/BCIP alkaline phosphatase substrate (Roche Molecular Biochemicals, Indianapolis, Indiana). Cryostat sections of frozen bovine testis were included as a positive control, and sense probes were included to determine nonspecific background labeling.

Immunohistochemistry

Eight-micrometer paraffin sections of bovine follicular and testis tissues were dewaxed and subjected to immunohistochemistry after the double peroxidase-antiperoxidase-avidin-biotin-complex protocol as previously described (33), with diaminobenzidine (Sigma UK Ltd) as chromogen. As primary antibody, the polyclonal antiserum (AS 33) raised in rats against a recombinant bovine pro-INSL3 protein made in *Escherichia coli* was

used, as previously described and validated (14), at a dilution of 1:1000. Sections were briefly counterstained using Light Green and mounted in aqueous mounting medium.

Statistical analysis

Real-time PCR data were analyzed as ΔCt values before conversion to fold difference values, and results were analyzed using 1- or 2-way ANOVA. Post hoc pairwise comparisons referred to in results were made by Fisher's protected least significant difference (PLSD) test. For in vitro experiments, results presented are combined data from 4 independent cultures. Statistical analysis of plasma hormone concentrations was performed by repeated measures ANOVA. Providing a significant "F" ratio was recorded post hoc Fisher's PLSD test was used for individual pairwise comparisons between different time points.

Results

Changes in INSL3 and RXFP2 mRNA expression in developing follicles and in CL

Mean Ct values for *ACTB* (β-actin), *INSL3*, and *RXFP2* were, respectively, 16.1, 16.8, and 25.5 for TIC, 15.3, 20.5, and 31.9 for GC, and 15.6, 21.3, and 33.4 for CL samples. As shown in Figure 1, the relative abundance of mRNA for *INSL3* and its receptor *RXFP2* was much greater in TIC than GC across all follicle size categories (2-way ANOVA effect of cell type: *INSL3*, $P < .001$; *RXFP2*, $P < .0001$). Levels of both transcripts varied significantly according to follicle size (2-way ANOVA effect of size class: *INSL3*, $P < .05$; *RXFP2*, $P < .001$). *INSL3*
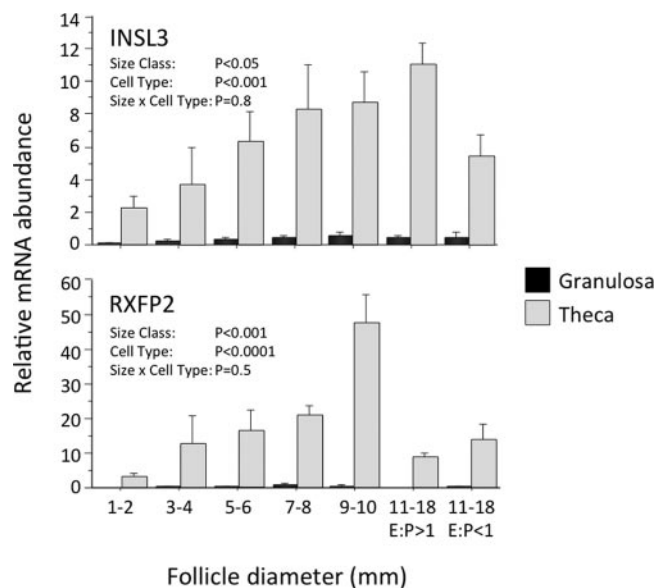

Figure 1. Relative abundance of mRNA transcripts for *INSL3* and its receptor *RXFP2* in the thecal and granulosal compartments of varying sizes of developing bovine antral follicles. Follicles in the largest size category (11-18 mm) were subdivided according to whether they were estrogen active, with an estrogen to progesterone ratio of greater than 1 (E:P > 1) or estrogen inactive (E:P < 1). Values are means ($\pm$SEM), and results of 2-way ANOVA are summarized.
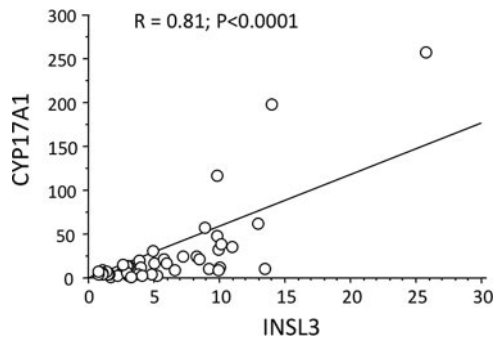
Figure 2. Correlation between the relative abundance of *INSL3* and cytochrome P450 17 alpha hydroxylase/17,20 lyase (CYP17A1) mRNA transcripts in the theca interna layer of developing antral follicles of 1-18 mm in diameter (n = 47); r = 0.81, $P < .0001$.

mRNA level in the TIC layer showed a progressive 5-fold increase as follicles developed from 1-2 to 11-18 mm and was greatest in the 11- to 18-mm estrogen-active follicles. Expression level was approximately 50% lower in estrogen inactive than estrogen-active follicles of this size category ($P < .05$; post hoc PLSD test). *RXFP2* expression in TIC also increased as follicles developed from 1–2 to 9–10 mm, before decreasing again in both estrogen-active and estrogen-inactive 11- to 18-mm follicles. There was a highly significant positive correlation (r = 0.81, $P < .001$, n = 47) between the relative mRNA abundance of *INSL3* and *CYP17* in the TIC compartment of follicles of 1–18 mm in diameter (Figure 2).

   INSL3 and *RXFP2* were also expressed in CL tissue (Figure 3), with the relative expression of *INSL3* being significantly higher in the midluteal stage than in regressing CL samples ($P < .05$). However, relative to β-actin, levels of *INSL3* mRNA were much lower in CL tissue than in follicular TIC samples (6- to 30-fold lower depending on follicle size class used for comparison).
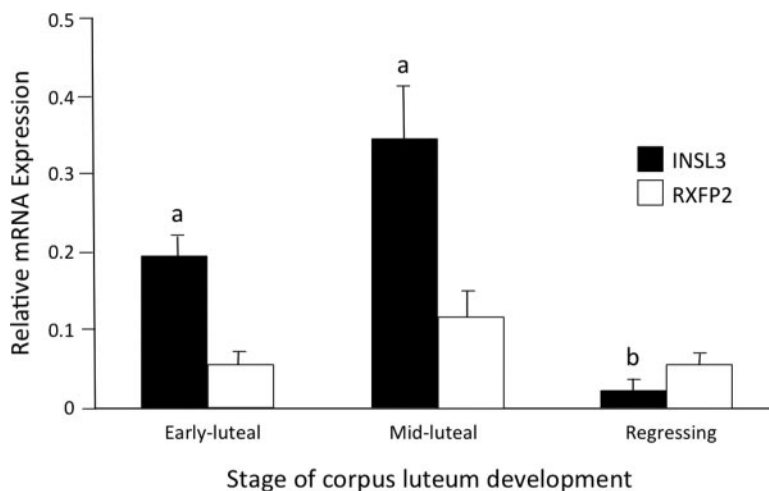
In situ hybridization: localization of INSL3 mRNA in ovary sections

   The mRNA expression data above showing that *INSL3* was mainly expressed in the thecal compartment was confirmed by in situ hybridization. Figure 4A shows that the intensity of staining for *INSL3* mRNA was much greater in the theca layer, with little staining in the GC layer or surrounding stromal tissue. The specificity of the hybridization probe for *INSL3* was confirmed by the absence of staining in the sense controls and by the specific staining of Leydig cells in testis sections, a cell type known to abundantly express INSL3 (2, 3).

Immunohistochemical localization of INSL3 protein in ovary sections

   The above quantitative PCR and in situ hybridization data were further confirmed by immunohistochemical staining of INSL3 protein. Figure 4B shows that the intensity of staining for INSL3 was much greater in the TIC layer, with little staining in the GC layer. The specificity of the antibody for INSL3 was confirmed by the specific staining of Leydig cells in testis sections.

In vitro TIC luteinization model

   The effect of exposing cultured bovine TIC to a luteinizing dose of LH on *INSL3* and *RXFP2* expression was examined. LH treatment for 4 days resulted in a more than 100-fold increase ($P < .001$) in the amount of progesterone secreted by the cells and a corresponding increase in the relative expression of transcripts for *STAR* ($P < .001$) and *P450SCC* ($P < .05$), indicative of functional luteinization (Figure 5). In contrast, LH-induced luteinization was associated with a marked decrease in the secretion of INSL3 protein ($P < .01$) and relative abundance of *INSL3* and *RXFP2* transcripts ($P < .01$ and $P < .001$, respectively).

Plasma steroid and INSL3 profiles during PG-synchronized estrous cycles

   Figure 6 shows mean daily plasma hormone profiles from 5 heifers (n = 15 cycles) sampled during PG-synchronized estrous cycles. Repeated measures ANOVA revealed a significant variation over time in plasma INSL3, E2, and P4 ($P < .001$), whereas plasma androstenedione levels did not vary significantly ($P = .35$). As expected, P4 levels fell steeply after PG, remaining low until
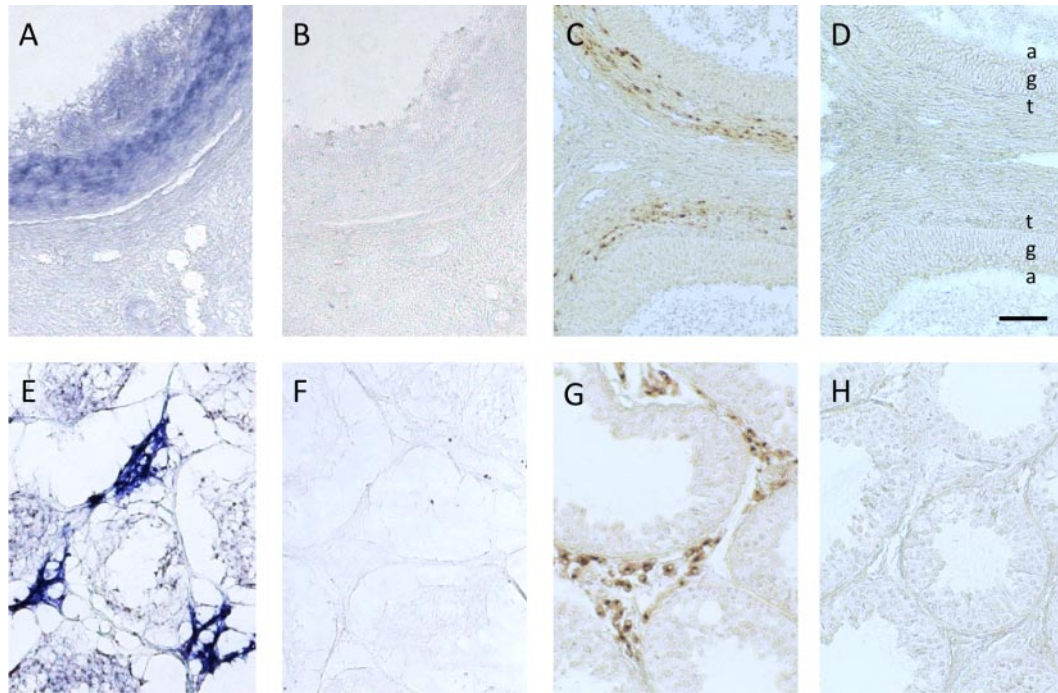

Figure 3. Comparison of the relative abundance of *INSL3* and *RXFP2* mRNA transcripts in bovine CL tissue. CL tissue was divided into early (n = 4), mid (n = 5), and late (n = 3) phase according to its morphology. Values are means (±SEM), and means indicated with different letters are significantly different ($P < .05$).

Figure 4. Localization of *INSL3* mRNA (in situ hybridization; blue staining) (A and E) and INSL3 protein (immunohistochemistry; brown staining) (C and G) in sections of bovine ovary (A–D) and testis (E–H) showing abundant expression in theca cells and Leydig cells, respectively. (B, D, F, and H) Corresponding control sections incubated with sense riboprobe or nonimmune serum. a, antrum; g, granulosa layer; t, thecal layer. Scale bar, 100 μm.

day 6 when the new CL was forming. Plasma E2 levels increased after PG induced luteolysis (d 0) and peaked on day 2–3, shortly before the preovulatory LH surge (d 3.5 ± 0.6). INSL3 levels followed a similar pattern to E2, in-

creasing by 38% ($P < .05$) from 62.9 pg/mL on day 0 to 86.6 pg/mL on day 2. Levels then fell by 54% to 39.8 pg/mL on day 4 ($P < .001$), coincident with the post-LH surge decline in E2.
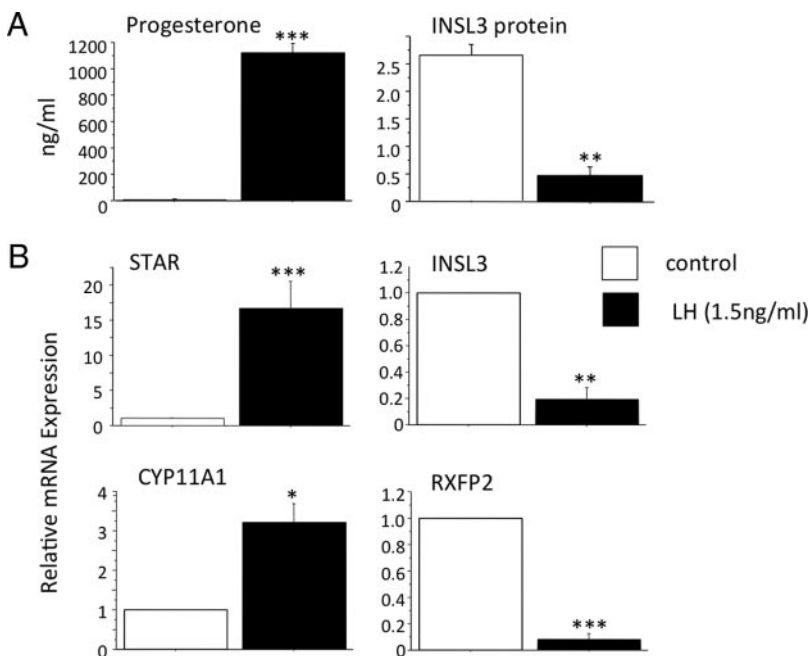
Does E2 directly alter expression of *INSL3* or *RXFP2* by nonluteinized TIC?

Given the above in vivo observation, we examined whether E2 could directly affect expression of INSL3 or its receptor RXFP2 by isolated TIC cultured under nonluteinizing conditions. As shown in Figure 7, treatment with E2 promoted a modest increase in androstenedione secretion (~50%; $P < .05$) but did not affect the relative abundance of *INSL3* or *RXFP2* transcripts.

Discussion

INSL3-null female mice have been shown to display impaired fertility (5, 17). However, there is a paucity of data regarding the ovarian expression pattern and potential role(s) of

Figure 5. Changes in (A) progesterone and INSL3 levels in conditioned media and (B) relative abundance of mRNA transcripts for steroidogenic acute regulatory protein (STAR), *CYP11A1*, *INSL3*, and *RXFP2* in bovine theca cells cultured 4 days with or without a luteinizing dose level of LH (1.5 ng/mL). Values are means (±SEM), and statistical analysis was performed by ANOVA.*$P < .05$, **$P < .01$, ***$P < .001$ (n = 4 independent culture experiments).
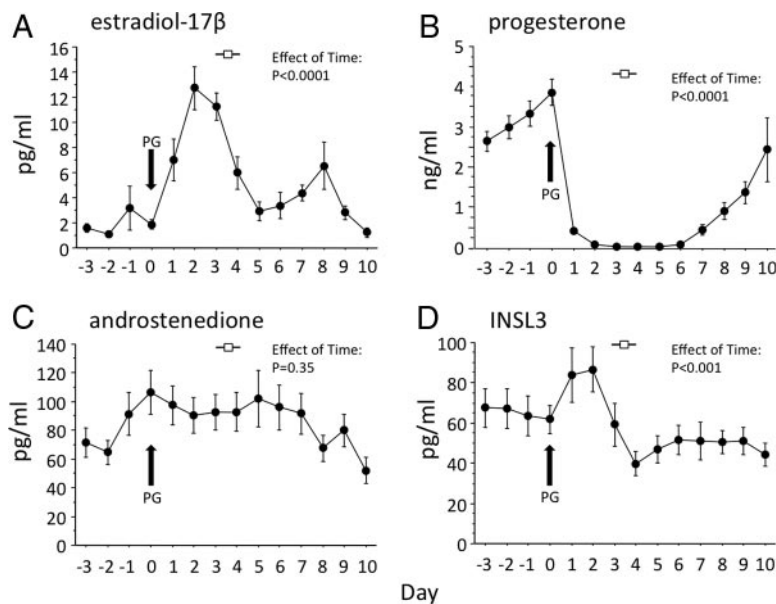
Figure 6. Changes in mean (±SEM) plasma concentrations of (A) E2, (B) progesterone, (C) androstenedione, and (D) INSL3 during PG-synchronized/shortened estrous cycles in heifers. Samples are aligned to the time of PG administration (d 0) indicated by the arrow. The mean (±SEM) time of the LH surge (d 3.5 ± 0.6) is indicated by the open square symbol. Statistical analysis was performed by repeated measures ANOVA.

INSL3-RXFP2 signaling in follicle development, steroidogenesis, and CL function. Given reports that the ovarian expression of INSL3 is considerably higher in ruminants than in nonruminant mammals (11, 18), in the first part of this study, we used real-time PCR to quantify the patterns of RNA expression for INSL3 and its receptor RXFP2 in the theca interna and granulosal compartments of developing bovine antral follicles and in early, midluteal, and regressing CL. Overall, the relative abundance of *INSL3* mRNA was found to be much greater in TIC than GC, an observation we confirmed by both in situ hybridization and by immunohistochemistry demonstrating expression at the translated protein level. This finding is consistent with previous studies showing that INSL3 is expressed predominantly by TIC (11, 14, 18). Our comparison of follicles of various size categories ranging from 1–2 to 11–18 mm revealed for the first time that *INSL3* expression increases progressively with follicle development, peaking in preovulatory stage follicles of 11–18 mm. Furthermore, when follicles of this size category were subdivided according to their E2 to P4 ratio (34), the *INSL3* transcript level was significantly lower (~50%) in the estrogen-inactive follicles (presumed to be regressing) than in the estrogen-active follicles (presumed to be healthy). The latter observation is consistent with an earlier report (14) that INSL3 expression levels were significantly decreased in atretic follicles. In the same study, pro-INSL3 protein was detected by immunohistochemistry in 100% of the small morphologically healthy follicles (2–5 mm) but in only 57% of morphologically healthy preovulatory follicles (12–17

mm) examined. It is unclear whether an absence of detectable staining reflects the limit of sensitivity of the method used or a genuine absence of translated INSL3 protein. A detailed immunohistochemical analysis of INSL3 expression at the protein level in follicles at different stages of development was beyond the scope of the present study.

We also found that expression of *RXFP2*, the cognate receptor for INSL3, was also substantially (~50-fold) higher in the thecal than granulosal compartment. Moreover, thecal *RXFP2* expression, like *INSL3*, showed a marked and progressive increase during follicle maturation. In contrast to *INSL3* levels, however, *RXFP2* levels peaked in 9- to 10-mm follicles, before declining approximately 5-fold in larger (11-18 mm) follicles, regardless of their estrogenic status. These novel findings on the intrafollicular distribution and pattern of change of *INSL3* and *RXFP2* expression support the concept that theca-derived INSL3 functions primarily as an autocrine/paracrine regulator of theca cell function. However, given that a substantial fall in *RXFP2* mRNA level was evident in large estrogen-active (11–18 mm) follicles expressing the highest levels of *INSL3* mRNA, this might imply that INSL3-RXFP2 signaling is actually maximal in the smaller 9- to 10-mm size class. Interestingly, acquisition of LH receptors by GC only occurs in bovine follicles growing beyond about 9 mm in diameter (35, 36), presaging their transition into estrogen-active preovulatory follicles capable of triggering, and ovulating in response to, an LH surge (37, 38).

Because estrogen-active preovulatory follicles have the greatest requirement for theca-derived androgen as an essential substrate for cytochrome P450 aromatase (39), one might expect that regulatory mechanisms conducive to sustained (or heightened) thecal androgen production would prevail in preovulatory follicles. Indeed, as reviewed elsewhere (40), a plethora of local factors have been identified as positive regulators of thecal androgen production, including IGF (41, 42), inhibin (43-45), and E2 itself (45, 46), the latter 2 produced in greatest amounts by GC of preovulatory follicles. Conversely, other intraovarian factors, including TGF-β (47), activins (44, 48), bone morphogenetic proteins (22, 24, 49), TNF-α (50), epidermal growth factor, and TGF-α (51), have been shown to suppress androgen produc-
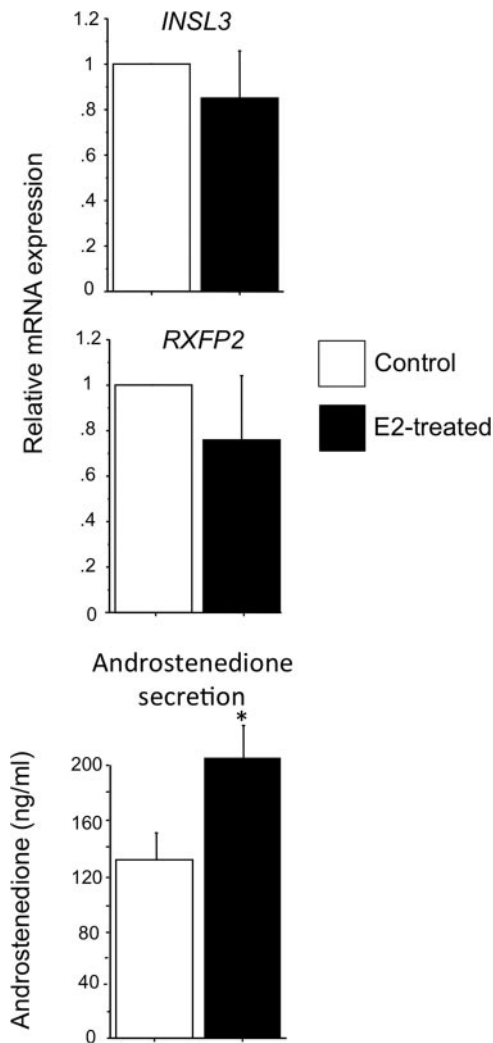
Figure 7. Lack of effect of E2 treatment (500 ng/mL) on relative expression of *INSL3* and *RXFP2* mRNA by bovine theca interna cells cultured in the presence of a nonluteinizing concentration of LH (150 pg/mL). Note that E2 significantly increased androstenedione secretion. Values are means, and bars indicate SEM (n = 4 independent cultures). *P < .05 versus control.

tion. This begs the question: Is there any evidence that INSL3-RXFP2 signaling contributes to the autocrine/paracrine regulation of thecal androgen production?

The much higher levels of expression of both *INSL3* and its receptor in the theca interna compartment in comparison with granulosal and luteal tissue suggest that INSL3 acts in an autocrine/paracrine manner within the follicle, being both predominantly produced by and acting upon TIC. In the male, an autocrine role for INSL3 has recently been described in mice, where both *INSL3* and *RXFP2* were found to be expressed in testicular Leydig cells. Treatment of cultured Leydig cells with INSL3 was found to stimulate testosterone and cAMP secretion (52). In the present study, *INSL3* mRNA expression was positively correlated with *CYP17A1* expression, whose gene product (cytochrome P450 17α- hydroxylase/17,20 lyase)

is a key enzyme responsible for conversion of progestins to androgens. Furthermore, in our cultured TIC model, addition of a luteinizing dose of LH, known to suppress androgen production by ovarian theca cells (53, 54), dramatically increased expression of *STAR* and *CYP11A1* mRNA and raised progesterone secretion concomitantly with reduced INSL3 secretion and reduced expression of *INSL3* and *RXFP2* mRNA. In addition, we have recently demonstrated (30) that RNA interference-mediated knock down of either INSL3 or RXFP2 expression in nonluteinized bovine TIC promotes a marked reduction in *CYP17A1* expression and androstenedione secretion. Collectively, these observations reinforce the notion that INSL3 is positively associated with follicular androgen production. Indeed, recent studies have found that INSL3 is elevated in the plasma of women with polycystic ovary syndrome and that levels in women with this syndrome are associated with ovarian hyperandrogenism (13, 20, 55).

INSL3 expression by bovine CL has been reported previously (11, 18, 21), but expression of its receptor *RXFP2* was not documented in these reports. In the present study, both *INSL3* and *RXFP2* mRNAs were detected in CL, although relative expression levels (normalized to β-actin) were, respectively, more than 10- and more than 100-fold lower than in TIC, perhaps indicating that functional INSL3-RXFP2 signaling is only weakly operational in CL tissue. Consistent with previous studies (11, 18), mean *INSL3* mRNA level was greatest in midluteal samples but declined more than 10-fold in regressing CL.

To corroborate the above findings of 1) increased TIC expression of *INSL3* during antral follicle development, 2) reduced *INSL3* mRNA expression in luteal tissue, and 3) reduced *INSL3* expression in TIC luteinized in vitro by exposure to high levels of LH, we used our novel bovine INSL3 immunoassay (21) to monitor, for the first time, circulating levels during PG-synchronized estrous cycles in cattle. We found a significant cyclic variation in plasma INSL3 concentrations during the bovine estrous cycle, with INSL3 following a similar profile to E2, increasing to maximal levels approximately 2 days after PG-induced luteolysis but then falling sharply after the ovulation-inducing LH surge on day 3–4 after PG injection. As expected, P4 fell steeply after PG induced luteolysis and did not rise again until 7 days later when a new CL was forming from the postovulatory follicle. It is notable that INSL3 levels did not fall in tandem with P4 after luteolysis, or rise with P4 during formation of the new CL. This further supports our finding that INSL3 is predominantly expressed by follicular theca interna cells of healthy preovulatory follicles, with much lower expression by CL. Taken together, these results strongly support the view that circulating INSL3 is a good biomarker for antral follicle development, at least during the first wave of a synchronized

cycle. In agreement with the finding of others (56, 57), plasma androstenedione levels did not vary significantly during the cycle, presumably because considerable amounts of the steroid present in the circulation emanate from follicles other than the dominant preovulatory follicle, and because some androstenedione is aromatized to estrogen. Further, some of the androstenedione in peripheral blood plasma is likely to be of adrenal origin. Finally, our observation that plasma INSL3 and E2 levels followed a similar profile after PG-induced luteolysis prompted us to examine whether direct exposure of cultured theca cells to E2, at a concentration comparable with intrafollicular concentrations in preovulatory follicles, could up-regulate INSL3 expression. Although E2 promoted a modest increase in androstenedione secretion, consistent with previous reports for cattle and human theca cells (45, 58), there was no effect on expression of *INSL3* or its receptor. Therefore, it remains to be investigated what the signal(s) are that lead to increased thecal *INSL3* expression during the latter stages of follicle development.

In conclusion, we have shown that much higher levels of INSL3 are produced by TIC than by the GC or CL and that expression levels increase progressively throughout antral follicle development. Moreover, follicular theca interna cells are the likely site of both production and action of INSL3 within the ovary. Our data indicate that cyclic changes in predominantly theca-derived INSL3, rather than CL-derived INSL3, likely from the dominant preovulatory follicle, are detectable in peripheral blood of cattle. Both in vitro and in vivo studies indicate that the expression of INSL3 is down-regulated during luteinization induced by the preovulatory LH surge. The positive correlation observed between *INSL3* and *CYP17A1* expression firmly indicates that INSL3 production within the ovary is linked to androgen production. Further investigation into the modulatory effects of INSL3 on thecal steroidogenesis will be of considerable interest, particularly in the context of ovarian androgen excess associated with conditions such as polycystic ovary syndrome.

Acknowledgments

References

1. **Adham IM, Burkhardt E, Benahmed M, Engel W.** Cloning of a cDNA for a novel insulin-like peptide of the testicular Leydig cells. *J Biol Chem*. 1993;268:26668–26672.

2. **Ivell R, Anand-Ivell R.** Biology of insulin-like factor 3 in human reproduction. *Hum Reprod Update*. 2009;15:463–476.

3. **Ivell R, Anand-Ivell R.** Biological role and clinical significance of insulin-like peptide 3. *Curr Opin Endocrinol Diabetes Obes*. 2011;18:210–216.

4. **Ivell R, Hartung S.** The molecular basis of cryptorchidism. *Mol Hum Reprod*. 2003;9:175–181.

5. **Nef S, Parada LF.** Cryptorchidism in mice mutant for Insl3. *Nat Genet*. 1999;22:295–299.

6. **Zimmermann S, Steding G, Emmen JM, et al.** Targeted disruption of the Insl3 gene causes bilateral cryptorchidism. *Mol Endocrinol*. 1999;13:681–691.

7. **Bathgate RA, Lin F, Hanson NF, et al.** Relaxin-3: improved synthesis strategy and demonstration of its high-affinity interaction with the relaxin receptor LGR7 both in vitro and in vivo. *Biochemistry*. 2006;45:1043–1053.

8. **Bogatcheva NV, Truong A, Feng S, Engel W, Adham IM, Agoulnik AI.** GREAT/LGR8 is the only receptor for insulin-like 3 peptide. *Mol Endocrinol*. 2003;17:2639–2646.

9. **Gorlov IP, Kamat A, Bogatcheva NV, et al.** Mutations of the GREAT gene cause cryptorchidism. *Hum Mol Genet*. 2002;11:2309–2318.

10. **Bamberger AM, Ivell R, Balvers M, et al.** Relaxin-like factor (RLF): a new specific marker for Leydig cells in the ovary. *Int J Gynecol Pathol*. 1999;18:163–168.

11. **Bathgate R, Balvers M, Hunt N, Ivell R.** Relaxin-like factor gene is highly expressed in the bovine ovary of the cycle and pregnancy: sequence and messenger ribonucleic acid analysis. *Biol Reprod*. 1996;55:1452–1457.

12. **Hanna CB, Yao S, Patta MC, Jensen JT, Wu X.** Expression of insulin-like 3 (INSL3) and differential splicing of its receptor in the ovary of rhesus macaques. *Reprod Biol Endocrinol*. 2010;8:150.

13. **Havelock JC, Bay K, Ivell R, Bathgate RA, Rodgers RJ, Carr BR.** A novel hormone known as insulin-like factor 3 (INSL3) is expressed in the human ovary and serum levels are increased in women with polycystic ovary syndrome (PCOS). *Fertil Steril*. 2005;84:S4 (Abstract).

14. **Irving-Rodgers HF, Bathgate RA, Ivell R, Domagalski R, Rodgers RJ.** Dynamic changes in the expression of relaxin-like factor (INSL3), cholesterol side-chain cleavage cytochrome p450, and 3β-hydroxysteroid dehydrogenase in bovine ovarian follicles during growth and atresia. *Biol Reprod*. 2002;66:934–943.

15. **Tashima LS, Hieber AD, Greenwood FC, Bryant-Greenwood GD.** The human Leydig insulin-like (hLEY I-L) gene is expressed in the corpus luteum and trophoblast. *J Clin Endocrinol Metab*. 1995;80:707–710.

16. **Zarreh-Hoshyari-Khah MR, Einspanier A, Ivell R.** Differential splicing and expression of the relaxin-like factor gene in reproductive tissues of the marmoset monkey (*Callithrix jacchus*). *Biol Reprod*. 1999;60:445–453.

17. **Spanel-Borowski K, Schäfer I, Zimmermann S, Engel W, Adham IM.** Increase in final stages of follicular atresia and premature decay of corpora lutea in Insl3-deficient mice. *Mol Reprod Dev*. 2001;58:281–286.

18. **Bathgate R, Moniac N, Bartlick B, Schumacher M, Fields M, Ivell R.** Expression and regulation of relaxin-like factor gene transcripts in the bovine ovary: differentiation-dependent expression in theca cell cultures. *Biol Reprod*. 1999;61:1090–1098.

19. **Bay K, Hartung S, Ivell R, et al.** Insulin-like factor 3 serum levels in 135 normal men and 85 men with testicular disorders: relationship to the luteinizing hormone-testosterone axis. *J Clin Endocrinol Metab*. 2005;90:3410–3418.

20. **Gambineri A, Patton L, De Iasio R, Palladoro F, Pagotto U, Pasquali R.** Insulin-like factor 3: a new circulating hormone related to luteinizing hormone-dependent ovarian hyperandrogenism in the polycystic ovary syndrome. *J Clin Endocrinol Metab*. 2007;92:2066–2073.

21. **Anand-Ivell R, Hiendleder S, Vinoles C, et al.** INSL3 in the ruminant: a powerful indicator of gender- and genetic-specific feto-maternal dialogue. *PloS One*. 2011;6:e19821.

22. **Glister C, Satchell L, Knight PG.** Changes in expression of bone morphogenetic proteins (BMPs), their receptors and inhibin co-receptor βglycan during bovine antral follicle development: inhibin can antagonize the suppressive effect of BMPs on thecal androgen production. *Reproduction*. 2010;140:699–712.

23. **Ireland JJ, Murphee RL, Coulson PB.** Accuracy of predicting stages of bovine estrous cycle by gross appearance of the corpus luteum. *J Dairy Sci*. 1980;63:155–160.

24. **Glister C, Richards SL, Knight PG.** Bone morphogenetic proteins (BMP) -4, -6, and -7 potently suppress basal and luteinizing hormone-induced androgen production by bovine theca interna cells in primary culture: could ovarian hyperandrogenic dysfunction be caused by a defect in thecal BMP signaling? *Endocrinology*. 2005;146:1883–1892.

25. **Glencross RG, Abeywardene SA, Corney SJ, Morris HS.** The use of oestradiol-17β antiserum covalently coupled to sepharose to extract oestradiol-17β from biological fluids. *J Chromatogr*. 1981;223:193–197.

26. **Glencross RG, Bleach EC, Wood SC, Knight PG.** Active immunization of heifers against inhibin: effects on plasma concentrations of gonadotrophins, steroids and ovarian follicular dynamics during prostaglandin-synchronized cycles. *J Reprod Fertil*. 1994;100:599–605.

27. **Bleach EC, Glencross RG, Feist SA, Groome NP, Knight PG.** Plasma inhibin A in heifers: relationship with follicle dynamics, gonadotropins, and steroids during the estrous cycle and after treatment with bovine follicular fluid. *Biol Reprod*. 2001;64:743–752.

28. **Glencross RG, Bleach EC, McLeod BJ, Beard AJ, Knight PG.** Effect of active immunization of heifers against inhibin on plasma FSH concentrations, ovarian follicular development and ovulation rate. *J Endocrinol*. 1992;134:11–18.

29. **Sauer MJ, Foulkes JA, Worsfold A, Morris BA.** Use of progesterone 11-glucuronide-alkaline phosphatase conjugate in a sensitive microtitre-plate enzymeimmunoassay of progesterone in milk and its application to pregnancy testing in dairy cattle. *J Reprod Fertil*. 1986;76:375–391.

30. **Glister C, Satchell L, Bathgate R, et al.** Functional link between bone morphogenetic protein and insulin-like peptide 3 signaling in modulating ovarian androgen production [published online March 25, 2013]. *Proc Natl Acad Sci USA*. doi:10.1073/pnas.1222216110.

31. **Kayani AR, Glister C, Knight PG.** Evidence for an inhibitory role of bone morphogenetic protein(s) in the follicular-luteal transition in cattle. *Reproduction*. 2009;137:67–78.

32. **Livak KJ, Schmittgen TD.** Analysis of relative gene expression data using real-time quantitative PCR and the 2(-Delta Delta C(T)) Method. *Methods*. 2001;25:402–408.

33. **Ivell R, Balvers M, Pohnke Y, et al.** A Immunoexpression of the relaxin receptor LGR7 in breast and uterine tissues of humans and primates. *Reprod Biol Endocrinol*. 2003;1:114.

34. **Ireland JJ, Mihm M, Austin E, Diskin MG, Roche JF.** Historical perspective of turnover of dominant follicles during the bovine estrous cycle: key concepts, studies, advancements, and terms. *J Dairy Sci*. 2000;83:1648–1658.

35. **Bao B, Garverick HA.** Expression of steroidogenic enzyme and gonadotropin receptor genes in bovine follicles during ovarian follicular waves: a review. *J Anim Sci*. 1998;76:1903–1921.

36. **Webb R, Nicholas B, Gong JG, et al.** Mechanisms regulating follicular development and selection of the dominant follicle. *Reprod Suppl*. 2003;61:71–90.

37. **Fortune JE, Rivera GM, Evans AC, Turzillo AM.** Differentiation of dominant versus subordinate follicles in cattle. *Biol Reprod*. 2001;65:648–654.

38. **Mihm M, Evans AC.** Mechanisms for dominant follicle selection in monovulatory species: a comparison of morphological, endocrine and intraovarian events in cows, mares and women. *Reprod Domest Anim*. 2008;43(suppl 2):48–56.

39. **Hillier SG.** Current concepts of the roles of follicle stimulating hormone and luteinizing hormone in folliculogenesis. *Hum Reprod*. 1994;9:188–191.

40. **Young JM, McNeilly AS.** Theca: the forgotten cell of the ovarian follicle. *Reproduction*. 2010;140:489–504.

41. **Magoffin DA, Kurtz KM, Erickson GF.** Insulin-like growth factor-I selectively stimulates cholesterol side-chain cleavage expression in ovarian theca-interstitial cells. *Mol Endocrinol*. 1990;4:489–496.

42. **Spicer LJ, Stewart RE.** Interaction among bovine somatotropin, insulin, and gonadotropins on steroid production by bovine granulosa and thecal cells. *J Dairy Sci*. 1996;79:813–821.

43. **Hillier SG.** Regulatory functions for inhibin and activin in human ovaries. *J Endocrinol*. 1991;131:171–175.

44. **Hsueh AJ, Dahl KD, Vaughan J, et al.** Heterodimers and homodimers of inhibin subunits have different paracrine action in the modulation of luteinizing hormone-stimulated androgen biosynthesis. *Proc Natl Acad Sci USA*. 1987;84:5082–5086.

45. **Wrathall JH, Knight PG.** Effects of inhibin-related peptides and oestradiol on androstenedione and progesterone secretion by bovine theca cells in vitro. *J Endocrinol*. 1995;145:491–500.

46. **Roberts AJ, Skinner MK.** Estrogen regulation of thecal cell steroidogenesis and differentiation: thecal cell-granulosa cell interactions. *Endocrinology*. 1990;127:2918–2929.

47. **Magoffin DA, Gancedo B, Erickson GF.** Transforming growth factor-β promotes differentiation of ovarian thecal-interstitial cells but inhibits androgen production. *Endocrinology*. 1989;125:1951–1958.

48. **Hillier SG, Yong EL, Illingworth PJ, Baird DT, Schwall RH, Mason AJ.** Effect of recombinant activin on androgen synthesis in cultured human thecal cells. *J Clin Endocrinol Metab*. 1991;72:1206–1211.

49. **Dooley CA, Attia GR, Rainey WE, Moore DR, Carr BR.** Bone morphogenetic protein inhibits ovarian androgen production. *J Clin Endocrinol Metab*. 2000;85:3331–3337.

50. **Andreani CL, Payne DW, Packman JN, Resnick CE, Hurwitz A, Adashi EY.** Cytokine-mediated regulation of ovarian function. Tumor necrosis factor α inhibits gonadotropin-supported ovarian androgen biosynthesis. *J Biol Chem*. 1991;266:6761–6766.

51. **Weitsman SR, Magoffin DA.** Transforming growth factor-α inhibition of luteinizing hormone-stimulated androgen production by ovarian theca-interstitial cells: mechanism of action. *Endocrine*. 1995;3:415–420.

52. **Pathirana IN, Kawate N, Büllesbach EE, et al.** Insulin-like peptide 3 stimulates testosterone secretion in mouse Leydig cells via cAMP pathway. *Regul Pept*. 2012;178:102–106.

53. **Komar CM, Berndtson AK, Evans AC, Fortune JE.** Decline in circulating estradiol during the periovulatory period is correlated with decreases in estradiol and androgen, and in messenger RNA for p450 aromatase and p450 17α-hydroxylase, in bovine preovulatory follicles. *Biol Reprod*. 2001;64:1797–1805.

54. **Voss AK, Fortune JE.** Levels of messenger ribonucleic acid for cholesterol side-chain cleavage cytochrome P-450 and 3β-hydroxysteroid dehydrogenase in bovine preovulatory follicles decrease after the luteinizing hormone surge. *Endocrinology*. 1993;132:888–894.

55. **Gambineri A, Patton L, Prontera O, et al.** Basal insulin-like factor 3 levels predict functional ovarian hyperandrogenism in the polycystic ovary syndrome. *J Endocrinol Invest*. 2011;34:685–691.

56. **Evans AC, Komar CM, Wandji SA, Fortune JE.** Changes in androgen secretion and luteinizing hormone pulse amplitude are associated with the recruitment and growth of ovarian follicles during the luteal phase of the bovine estrous cycle. *Biol Reprod*. 1997;57:394–401.

57. **Peterson AJ, Fairclough RJ, Smith JF.** Radioimmunoassay of androstenedione and testosterone in cow plasma at the time of luteolysis and oestrus. *J Reprod Fertil*. 1978;52:127–129.

58. **Gilling-Smith C, Willis DS, Franks S.** Oestradiol feedback stimulation of androgen biosynthesis by human theca cells. *Hum Reprod*. 1997;12:1621–1628.